J Mater Sci (2009) 44:1121–1126
DOI 10.1007/s10853-008-3178-9

Titanium diboride–nickel graded materials prepared by field-activated, pressure-assisted synthesis process

Shao Ping Chen · Qing Sen Meng · W. Liu · Z. A. Munir

Received: 25 November 2007 / Accepted: 9 December 2008 / Published online: 22 January 2009

Abstract The formation of four-layered functionally graded material (FGM) samples of TiB_2–Ni/TiB_2–Ni_3A + Ni/Ni_3Al/Ni by field-activated, pressure-assisted synthesis process (FAPAS) was investigated. The microstructure, phase composition of the interfaces, and mechanical properties of the graded material were characterized. Elemental concentration profiles across interfaces between layers showed significant interdiffusion, indicative of formation of good bonds. The measured microhardness values of the sample increased monotonically from the nickel substrate to the surface layer (TiB_2–Ni). The values ranged from about 360 to over 3500 HK over a distance of 2 mm. The results of this investigation demonstrate the feasibility of the FAPAS process for rapid formation of FGMs with good diffusion bonds.

Introduction

Functionally graded materials (FGMs), as a kind of advanced materials, have more excellent performance than normal homogeneous ones in special work condition because of their flexible change in microstructure, composition, and structure in geometric space and are prospective in the field of engineering. The recognition that residual stress at the interface between materials with significantly dissimilar physical properties leads to unsatisfactory performance, has led to the concept and subsequent design of graded interfaces in various applications [1–6]. The FGMs were initially designed to ameliorate stress build up in thermal barrier coatings (TBCs) and has been utilized in various other applications. Formation of a graded interface has been accomplished by a variety of methods, including centrifugation [7, 8], sintering or reactive sintering of layered powders with graded composition [9–11], and self-propagating high-temperature synthesis (SHS) [12, 13].

In this work we have used the field-activated, pressure-assisted synthesis process (FAPAS) because of its ability to accomplish fast low-temperature consolidation, a circumstance that overcomes the problem of grain growth effectively. Since the reaction between Al and Ni is not sufficiently exothermic, the use of the SHS method is not suitable for the formation of the intermetallic that will be part of the gradation in our system. However, such reactions can be activated by other methods either prior to the reaction, e.g., through milling or preheating the reactants, or during the reaction, e.g., by the application of an electric field [14]. A modification of field activation is the FAPAS process which involves the application of a uniaxial pressure along with the electric field [15]. The advantages of the simultaneous application of an electric field (current) and a uniaxial pressure to consolidate or synthesize consolidate materials have been discussed in a recent review [16].

It was aimed in this paper that producing a titanium diboride–nickel graded materials starting with the base layer of Ni and coated by a layers of TiB_2–(Ni_3Al + Ni) composite and TiB_2–Ni composite. Nickel aluminide

S. P. Chen · Q. S. Meng (✉) · W. Liu
College of Material Science and Engineering,
Taiyuan University of Technology, 79 West Yingze St.,
Taiyuan 030024, China
e-mail: mengqingsen@263.net;
mengqingsen1950@yahoo.com.cn

S. P. Chen
e-mail: sxchenshaoping@163.com

Z. A. Munir
Department of Chemical Engineering and Materials Science,
University of California, Davis, CA 95616, USA
e-mail: zamunir@ucdavis.edu

(Ni_3Al) was chosen because of the small difference between its thermal expansion coefficient and those of the TiB_2–Ni composite and the nickel base layer. In addition, Ni_3Al has high creep strength and toughness. Titanium diboride is a refractory compound with high electrical and thermal conductivities; it possesses high hardness (microhardness 3250 HK), good fracture toughness (6.2 MPa $m^{1/2}$ at 20 °C), good corrosion resistance, and good wettability by liquid nickel metals [17, 18].

Experimental materials and methods

The starting materials in this study included powders of nickel, aluminum, TiB_2, and substrates of Ni wafers. The Ni and Al powders were 99.9% pure and have a particle size in the range 1–5 μm. The TiB_2 powders had a sieve classification of −325 mesh. All powders were obtained from Johnson-Matthey (Ward Hill, MA). The nickel substrates were in disk form, 18.9 mm in diameter and 1 mm thick.

The reactants were assembled in four layers, shown schematically in Fig. 1. The top layer is a mixture of TiB_2 and Ni powders ($30TiB_2 + 70Ni$, wt%). The second layer is a mixture of TiB_2, Ni, and Al powders in proportions of $30TiB_2 + 65Ni + 5Al$, wt%. The third layer is a mixture of Ni and Al powders with a molar ratio of 3:1. The fourth layer is the substrate of nickel substrate.

Powders of the first, second, and third layers were mixed separately in a glass ball milled for 1–2 h to ensure uniformity. Then each powder mixture was cold-pressed into thin disks, 18.9 mm in diameter with a relative density of 60%. The thicknesses of the layers were: 0.5, 0.5, and 0.3 mm for the first, second, and third layers, respectively. The powder disks and the nickel substrate were placed between two graphite punches in a cylindrical die of the FAPAS apparatus.

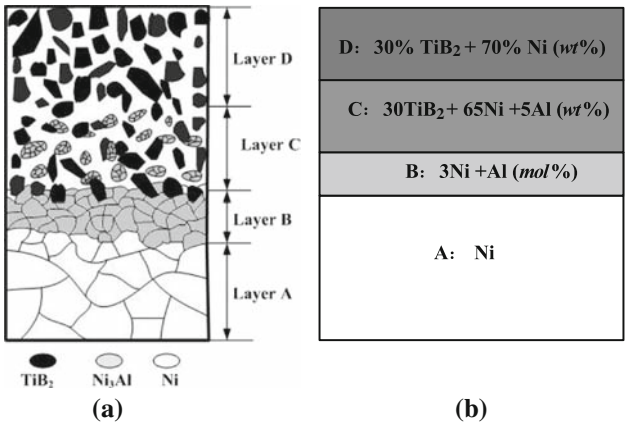

Fig. 1 Schematic diagram of **a** FGM and **b** reactant layers

The FAPAS apparatus consisted of a 100 kN pressure and a power supply capable of producing an AC current of up to 1750 A at 10 V. Temperatures were measured by a W-5%Re-W-26%Re thermocouple (OMEGA, diameter 0.3 mm), which was inserted in the side of the graphite die, as shown schematically in Fig. 2.

The formation of the FGM was accomplished under a vacuum of about 2×10^{-4} Pa. Typical real-time profiles of electric current and temperature are shown in Fig. 3. By adjusting the current, the sample was initially heated to 980 °C in 7 min and held at this temperature for 7 min under a current of about 1400 A and a load of 70 MPa. The temperature was then decreased to 850 °C and held for 5 min. Following this, the sample was cooled at a rate of 70 °C per minute to 500 °C, at 20 °C per minute to 300 °C, then at 20 °C per minute to 80 °C. A controlled cooling speed is employed to minimize residual stress and eliminate microcracking at the interfaces between layers.

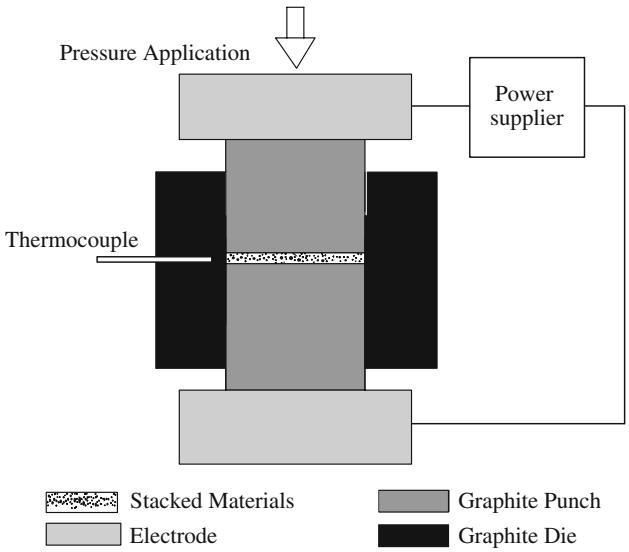

Fig. 2 Schematic diagram of the FAPAS apparatus

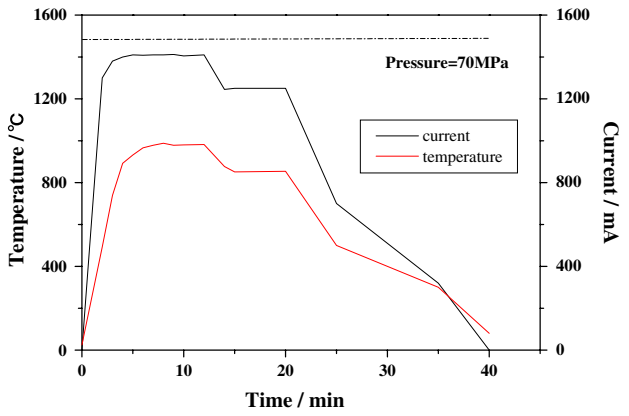

Fig. 3 Relation curve of electric current, temperature versus time

Following consolidation, the samples were cross-sectioned and the microstructure and phase composition were determined by scanning electron microscopy (SEM, FEI XL30-SFEG), optical microscopy (NIKON 6 V), and X-ray diffraction analysis (XRD, RIGAKU, 40 KV, 100 mA). The Knoop hardness of each layer of the sample was also evaluated (LECO, M-400-H1).

Results and discussion

Analysis of the graded structure

After sintering, four-layered materials of stock got bonded completely with its adjacent two layers to form as a unit by diffusion and interlocking and any cracking and defects were not observed. SEM image of the typical cross-section of a sample is shown in Fig. 4. Four layers can be observed in the sample and the EDS results showed that layer A is the nickel substrate, layer B is the intermetallic Ni_3Al, layer C is TiB_2–Ni_3Al + Ni composite, and layer D is TiB_2–Ni composite.

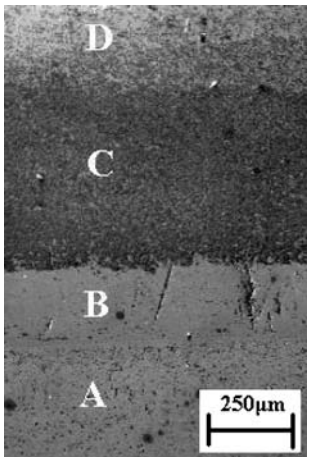

Fig. 4 Graded structure of the sample. A—nickel substrate, B—layer B of Ni_3Al, C—layer C of $(TiB_2)_p(Ni_3Al + Ni)$, D—layer D of $(TiB_2)_pNi$

Figure 5, a back-scattered SEM image, reveals the nature of the bond between the nickel substrate and the intermetallic compound Ni_3Al layer and shows a transition region between the layers of about 13 μm thickness. In fact, the transitional layer is a diffusion dissolute one formed by mutual diffusion of aluminum atoms and nickel atoms of layer B and layer A, respectively driven by thermodynamic potential gradient, which owns to the imposition of the electric field on the materials and the reaction heat of nickel powder and aluminum powder to form Ni_3Al in the layer B. On the one hand, the imposition of field will increase the concentration of vacancies and reduce the mobility activation energy for defects [19, 20], which will improve the mass transport in the interface of different materials. On the other hand, the reaction heat will make the temperature raised and increase the amount of atoms that may cross the potential barrier and the concentration of vacancies subsequently. Both the electric field and reaction heat promotes the atoms to migrate across the interface. Concentration profiles, Fig. 5b, of Al and Ni across the transition layer show significant interdiffusion, indicative of formation of a good bond between Ni_3Al and Ni which have similar face-centered cubic structure and lattice parameters.

The microstructure of layers B and C is shown in Fig. 6. The part at right side is single phase with homogeneous grains and that at the left side is composite with light matrix reinforced by black particles well distributed. The EDS analysis results of layer C shows that they are TiB_2

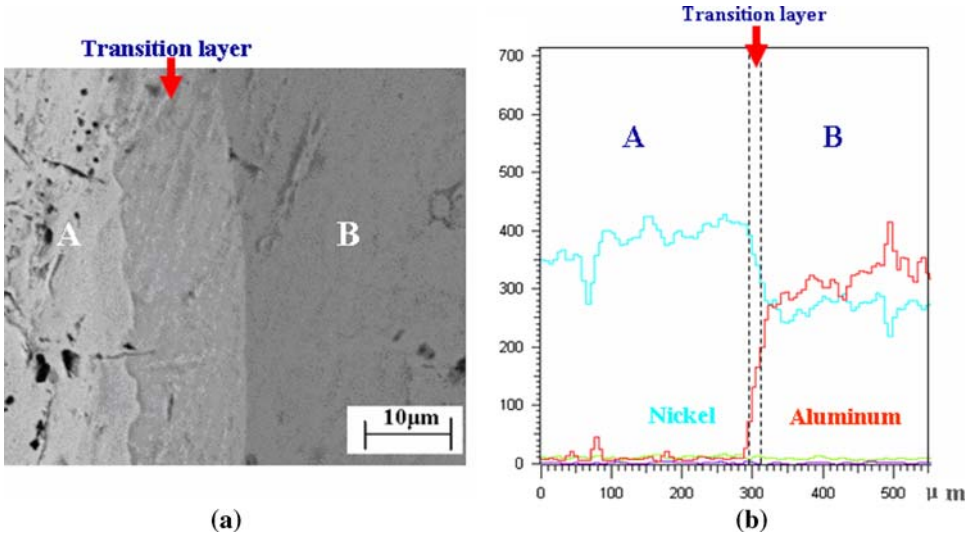

Fig. 5 Microstructure and EDS analysis of the interface of A–B. **a** Detail of the interface between layer A and layer B. **b** EDS analysis of the interface of A–B

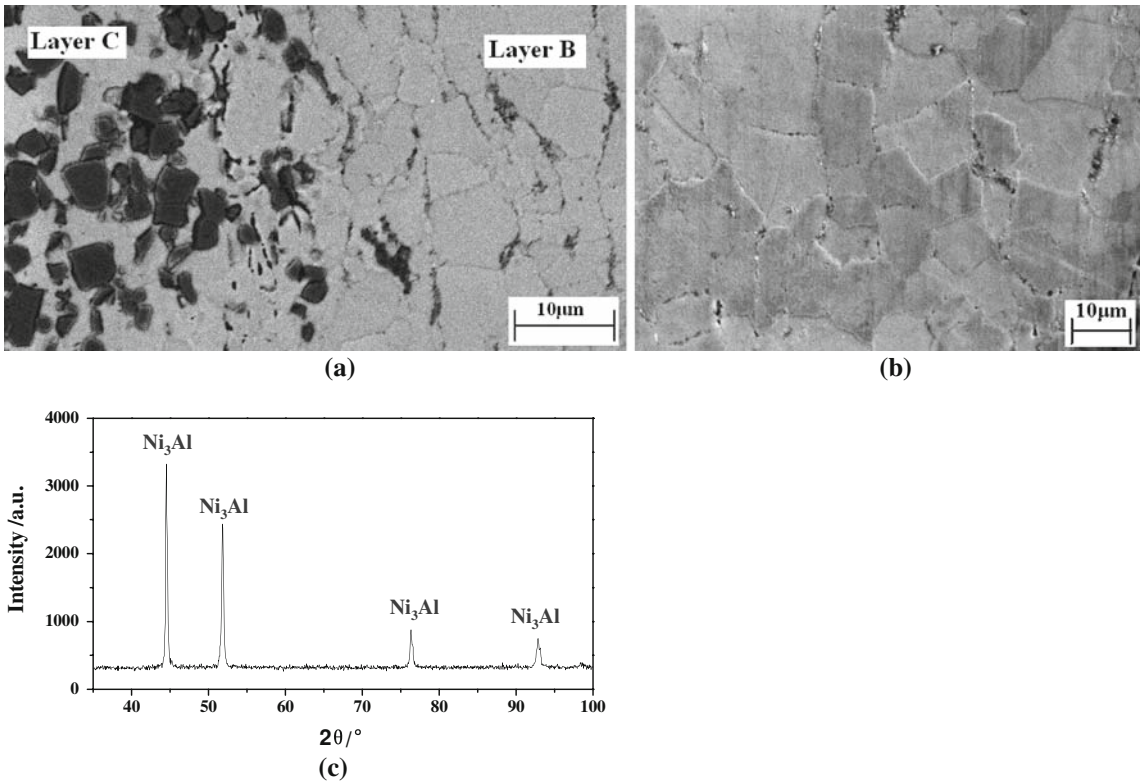

Fig. 6 Microstructure and XRD analysis results of layer B, layer C, and their interface. **a** Details of the interface of layer B and layer C by back scattered SEM. **b** Microstructure of the Ni_3Al intermetallic of layer B. **c** XRD analysis results of layer B

and nickel, respectively, which are not shown here. The two layers were bonded very well to form a unit and no evident dividing line between them is observed (Fig. 6a). Figure 6b shows the microstructure of the layer B which consists only one single phase after sintering. The X-ray diffraction (Fig. 6c) analyses of this layer showed the presence of the intermetallic Ni_3Al and its average grain size is 5–7 μm, no any residual powder of nickel or aluminum or other compound was detected. So it can be indicated that the initial powder mixture of the layer B made a full reaction to form Ni_3Al under the condition of FAPAS. Because the combination of Ni and Al is exothermal reaction, a great deal of heat will be produced which will make the temperature raised and promote the preparation of FGMs.

The microstructure and XRD results of layers C and D are shown in Fig. 7. The transition between layers C and D is seen in Fig. 7a. The dark phase in Fig. 7b represents TiB_2, the light region represents Ni, and the light gray region (indicated by the arrow) represents a mixture of Ni and Ni_3Al, as was determined from the XRD results shown in Fig. 7c. The presence of Ni_3Al in the layer C improved the bonding between layers B, C, and D, and increased the microhardness of layer C significantly, as will be seen later. The microstructure of layer D is shown in Fig. 7d. Particles of TiB_2 appear to be well bonded with Ni and Ni_3Al and there is no evidence of micro-cracking or cavity formation, due to the good wettability of TiB_2 by liquid Ni.

Mechanical properties of the sample

Results of the microhardness measurements across the layers are shown in Fig. 8. There is a gradual increase in hardness from the nickel substrate to the surface layer of D. The microhardness increases from about 360 to over 3500 HK over a distance of 2 mm. The measured values exhibited considerable scatter in layers C and D, which is a consequence of the composition in the tested area and the size of the grains relative to the spot size of the measurement. The grains of TiB_2 varied in size from 2 to 10 μm and as can be seen from Fig. 7, thus the higher hardness values are likely a reflection of the contribution of the titanium diboride phase.

The tests of thermal shock resistance were carried out in order to evaluate the bonding strength of each layer. The sintered specimens were heated to 600 °C initially and then put into the water in temperature of 20 °C at once. The process was repeated for 20 times. Following the test, samples were examined by optical microscopy and the

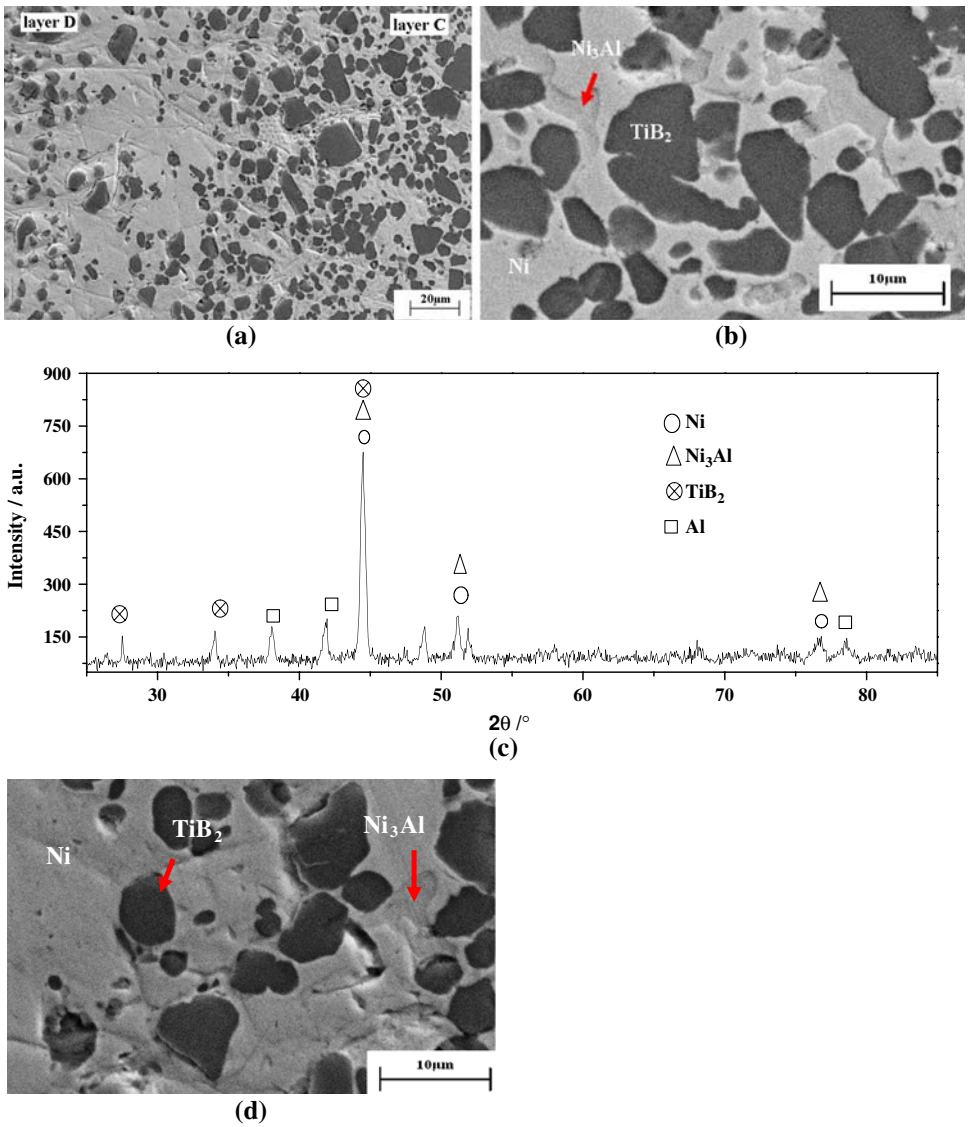

Fig. 7 Microstructure and XRD analysis of the layer C and layer D. **a** Microstructure of layer C and layer D. **b** Details of the layer C (Ni + Ni_3Al)–matrix composite. **c** XRD analysis of the layer C. **d** Details of the layer D (Ni)–matrix composite, a little of Ni_3Al can be observed near the layer C shown by the arrow

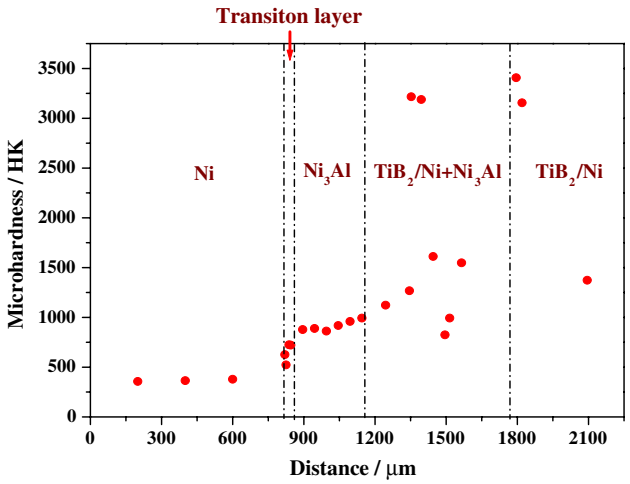

Fig. 8 Microhardness distribution across the sample

results showed the absence of cracks at the interfaces between the layers.

Conclusions

An FGM of TiB_2 + Ni/TiB_2 + Ni_3Al + Ni/Ni_3Al/Ni was produced by the FAPAS process by simultaneously reacting and consolidating powders of Ni, Al, and TiB_2 placed on top of Ni substrate. The microstructure of the interfaces between the resulting layers and concentration profiles of elements across the interfaces show good bonding between the layers. The results of the microhardness measurements show a gradual increase from the nickel substrate to the surface layer D (TiB_2 + Ni). Over this range, which is about 2 mm thick, the microhardness increased from about 360 to over 3500 HK. The hardness of the composite

surface layer showed considerable scatter in the layer C and D reflecting compositional variation and spot size of the measured regions. The test of thermal shock showed that the adjacent layers had good bonding strength.

Acknowledgements This study works were supported by the projects of the NSFC of China (50671070). The work was also partially supported by a grant from the Army Office of Research (ZAM).

References

1. Kieback B, Neubrand A, Riedel H (2003) Mater Sci Eng A 362:81
2. Koizumi M (1997) Int J Self-Propag High-Temp Synth 6:295
3. Lee CS, Zhang XF, Thomas G (2001) Acta Mater 49:3775
4. Zhu S, Wlosinski W, Xu B (2003) Mater Sci Forum 423–425:293
5. Anne G, Vanmeensel K, Vleugels J, Van der Biest O (2006) Key Eng Mater 314:213
6. Muller E, Drasar C, Schilz J, Kaysser WA (2003) Mater Sci Eng A 362:17
7. Meng QS, Chen SP, Munir ZA et al (2007) Mater Sci Eng A 456:332
8. Meng QS, Chen SP, Munir ZA et al (2008) Key Eng Mater 368–372:1876
9. Meng QS, Liu CR, Munir ZA et al (2008) J Mater Sci 43:5076. doi:10.1007/s10853-008-2583-4
10. Carrillo-Heian EM, Gibeling JC, Munir ZA, Paulino GH (2001) Ceram Trans 114:241
11. Reddy BSB, Das K, Das S (2007) J Mater Sci 42:9366. doi:10.1007/s10853-007-1827-z
12. Fu ZY, Liu JP, Zhang JY, Zhang QJ (2003) Key Eng Mater 249:105
13. Roine A (1999) Outokumpu HSC chemistry for Windows: chemical reaction and equilibrium software with extensive thermochemical database. Version 4.0. Outokumpu Research Oy, Finland, ISBN 952-9507-05-4A
14. Heian EM, Munir ZA (2002) Ceram Trans 135:61
15. Carrillo-Heian EM, Carpenter RD, Paulino GH, Gibeling JC, Munir ZA (2001) J Am Ceram Soc 84:962
16. Munir ZA, Anselmi-Tamburini U, Ohyanagi M (2006) J Mater Sci 41:763. doi:10.1007/s10853-006-6555-2
17. Shi CX, Li HD, Zhou L (2004) The handbook of material science and engineering (in Chinese). Chemical Industry Press, Beijing, p 132
18. Lide DR, Kehiaian HV (1994) CRC handbook of thermophysical and physicalchemical date. CRC Press, Boca Raton, p 788, 208
19. Asoka-Kumar P, Alatalo M, Gosh VJ, Kruseman AC, Nielson B, Lynn KG (1996) Phys Rev Lett 77:2097
20. Garay JE, Glade SC, Anselmi-tamburi U, Asoka-Kumar P, Munir ZA (2004) Appl Phys Lett 85:573